Design and performance test of a combined and adjustable precise rice seed metering device

Hongmei Xu[1,2], Wanru Liu[1,2], Hao Liu[1,2], Zhangfen Liu[1,2], Guozhong Zhang[1,2*]

(1. *College of Engineering, Huazhong Agricultural University, Wuhan 430070, China*;
2. *Key Laboratory of Agricultural Equipment in Mid-lower Yangtze River, Ministry of Agriculture and Rural Affairs, Huazhong Agricultural University, Wuhan 430070, China*)

Abstract: In order to address the issues of narrow seeding adjustment range and low accuracy of grain placement in the existing rice seeders, a mechanically and pneumatically adjustable precision hole-type seeder is designed. It is primarily composed of a seeding disk, air chamber, seed box, and seed discharge device. The design incorporates a symmetrical structure with dual disks and dual casings, enabling both single-sided and double-sided single-row and synchronized seeding. Based on theoretical analysis of seed charging, seed protection, and seed release, the following parameters were determined: seeding disk diameter of 192 mm, suction hole diameter of 1.48-1.52 mm, suction hole spacing of 3.04-9.41 mm, type hole distribution circle radius of about 62.1-77.0 mm, type hole diameter of 9 mm, stirrer plate length of 4.705-9.410 mm, and stirrer plate inclination angle of 0°-30°. Using a coupled simulation method of EDEM-Fluent, the impact of different type hole distributions, stirrer plate lengths, and inclination angles on seeding performance was analyzed. The results indicate that the main and secondary influencing factors on seed charging qualification rate are type hole diameter, stirrer plate inclination angle, and stirrer plate length. The optimal performance is achieved with a type hole diameter of 6 mm, stirrer plate length of 5 mm, and stirrer plate inclination angle of 10°, resulting in a seed charging qualification rate of 71.42%. Furthermore, Fluent software was utilized to analyze the influence of different suction hole spacings, diameters, and air chamber radii on seeding performance. The results revealed that the suction of rice seeds by the hole can be better realized with a suction hole spacing of 6 mm, a suction hole diameter of 1.5 mm, and an air chamber radius of 62 mm, at which the average negative pressure in the suction hole center was about 2824.56 Pa. A bench test and a field test were further performed on the device. The results showed that increasing the number of type holes and suction holes can contribute to more stable regulation of the seeding amount. The optimal single-sided seed metering could achieve a maximum qualified rate of 82.5%, a missing rate of 12.5%, and a repeating rate of 5%; while the optimal double-sided seed metering could obtain a maximum qualified rate, missing rate, and repeating rate of 72.5%, 15%, and 12.5%, respectively. This adjustable precision seeder can meet the requirements of precision sowing of Huanghuazhan rice varieties, and the research findings can provide reference for the structural optimization of precision rice seeders.

Keywords: rice, combined seed metering device, adjustable seeding amount, EDEM-Fluent
DOI: 10.25165/j.ijabe.20251801.8193

Citation: Xu H M, Liu W R, Liu H, Liu Z F, Zhang G Z. Design and performance test of a combined and adjustable precise rice seed metering device. Int J Agric & Biol Eng, 2025; 18(1): 101–114.

1 Introduction

Mechanized direct seeding is one of the important directions of rice planting in China. Currently, the rice varieties widely planted in China can be mainly divided into hybrid and conventional rice with strong tillering ability, with the former requiring 3-5 seeds/hole and the latter requiring 3-8 seeds/hole in direct seeding[1]. Therefore, there is an urgent need for seeders and/or tools with adjustable seeding amounts for different rice varieties.

The rice seed metering device is the core component of the direct seeding system[2], which can be divided into mechanical and pneumatic types[3] according to its principle. Some research has been carried out on the adjustment of seeding amount by mechanical and pneumatic rice seed metering devices. For example, Liu et al.[4] designed a spiral groove wheel seed metering device, which controls the spiral groove length by adjusting the baffle to regulate the seeding amount. Li et al.[5] designed an electromagnetic vibration precise rice seed metering device by combining the outer-groove-wheel seed metering and electromagnetic vibration seed metering, with the latter to control sowing amount and precision. According to the precision agronomic requirements of rice sowing, Zhang et al.[6] designed a seed metering device with a wheel equipped by large and small type holes, and realized the regulation of seeding amount by coordinating the wheel shell and holes. Zhang et al.[7] designed a double-cavity rice seed metering device with curved bristles, in which a single cavity is used for seeding hybrid rice and double cavities are used for seeding conventional rice. Xing et al.[8] constructed a pneumatic seed metering device with adjustable seeding amount, which is equipped with runners of multiple negative pressure and can adjust the seeding amount by the switch of the runner.

At present, great progress has been made in the research on rice

Received date: 2023-03-03 **Accepted date:** 2024-02-18
Biographies: **Hongmei Xu**, PhD, Professor, research interest: agricultural equipment and intelligent technology, Email: xuhongmei@mail.hzau.edu.cn; **Wanru Liu**, PhD candidate, research interest: agricultural machinery, Email: liuwanru@webmail.hzau.edu.cn; **Hao Liu**, MS, research interest: agricultural machinery, Email: liuhao20789@163.com; **Zhangfen Liu**, MS, research interest: agricultural machinery, Email: 1021465716@qq.com.
***Corresponding author: Guozhong Zhang**, PhD, Professor, research interest: agricultural machinery. Huazhong Agricultural University, Wuhan 430070, China. Tel: +86-18672783365, Email: zhanggz@mail.hzau.edu.cn.

precise seeding, which provides some reference for the design of precise rice seed metering devices. On the basis of the above findings and the agronomic requirements of precise direct seeding of rice, this study designed an adjustable rice seed metering device by combining mechanical and pneumatic means. The device can realize seeding-amount-adjustable unilateral seeding or bilateral seeding for different rice varieties. Finally, by EDEM-Fluent coupling simulation, bench test, and field test, the key structural parameters such as the type hole, suction hole, and stirring plate were optimized to ensure adjustable precise rice seed metering.

2 Structure and working principle of the rice seed metering device

2.1 Structure of the rice seed metering device

As shown in Figure 1, the rice seed metering device is mainly composed of two seeding plates, two air chambers, two shells, two seed discharging devices, two type hole cleaning brushes, two suction hole cleaning brushes, two seeding boxes, type holes with seed stirring plates, and suction holes in a symmetrical manner. The device is of a symmetrical structure connected with the shaft through flanges. Mechanical and pneumatic seeding are combined. The double working principles consist of mechanical seed filling and gravity seed discharge of the mechanical device and negative-pressure seed filling and positive-pressure seed discharge of the pneumatic device, thereby realizing unilateral type hole and/or suction hole, unilateral type hole + bilateral suction hole, bilateral type hole + unilateral suction-hole, and bilateral type hole + bilateral suction hole rice seed metering.

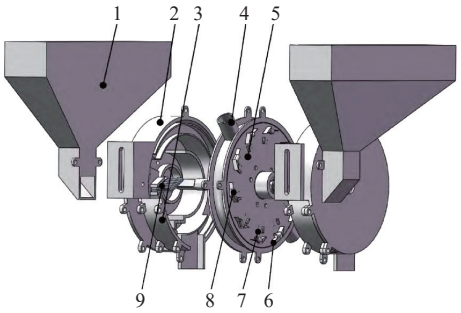

1. Seed box; 2. Shell; 3. Seed discharge device; 4. Air chamber; 5. Seeding plate; 6. Type hole stirring plate; 7. Suction hole; 8. Type hole; 9. Clearing brush

Figure 1 Schematic diagram of the combined adjustable rice precise seed metering device

2.2 Seeding process of the rice seed metering device

As shown in Figure 2, when working, the seeding plate rotates clockwise along with the axis, and the stirring plate and the long stirring teeth on the type hole continuously stir the rice seeds. Under the combined action of the stirring plate and their own gravity, the discrete rice seeds enter the type hole. The air chamber connected to the negative-pressure fan forms a negative-pressure chamber to suck rice seeds to the suction hole. The position of the negative-pressure chamber on the rice seed metering device is shown in Figure 3. The rice seeds entering the type hole and the suction hole continue to rotate with the seeding plate. The clearing brush of the type hole removes excess seeds accumulated in the type hole, and the clearing brush of the suction hole removes excess seeds sucked by the suction hole to complete the seed clearing process. The removed seeds flow back to the seed filling chamber to continue participating in the subsequent seeding. The type hole and suction hole after seed clearing are rotated to the seed protection area, and an arc plate is designed according to the seed movement path. The seed protection groove on the arc plate forms a seed protection channel with the seeding plate on both sides of the type hole, so as to ensure that rice seeds do not break away from the type hole. The suction hole on the seeding plate is continuously connected with the negative-pressure chamber to ensure that the rice seeds do not break away from the suction hole and complete the seed protection process. When the seeding plate rotates to the seeding area, the type hole is separated from the seed protection channel, and the seeds are released from the type hole under the action of gravity and centrifugal force. At this time, the suction hole also enters the operating range of the positive-pressure air chamber, and rice seeds are released from the suction hole under the combined action of their own gravity and positive pressure, completing the seeding process. The positive-pressure air chamber is connected with the positive-pressure fan or the outside air; the position of the positive-pressure air chamber is shown in Figure 3. Because the type hole and suction hole of the seeding plate can independently complete seed filling, seed clearing, seed protection, and seed casting, the seeding plate can realize multi-stage and multi-displacement regulation of rice seeding through independent or joint operation of the mechanical and pneumatic seeding plate.

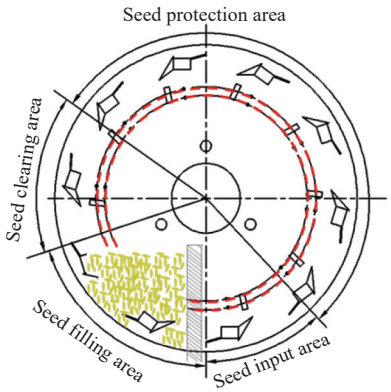

Figure 2 Schematic diagram of the working process of the rice seed metering device

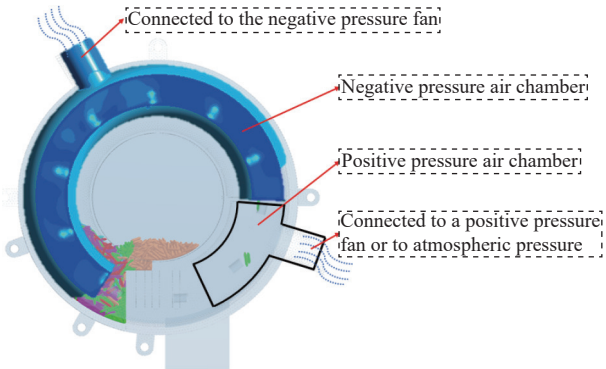

Figure 3 Schematic diagram of positive-pressure chamber and negative-pressure chamber

3 Structure design and process analysis of the rice seed metering device

3.1 Structure design

The seed filling performance of the device can be improved by increasing the contact area between rice seeds and type hole in the filling chamber, rice seed mobility, and the filling time. In addition, increasing the number of type holes and suction holes can increase

the seeding frequency, but an excessive number of type holes and suction holes will lead to an increase in the diameter of the seeding plate, resulting in the increase in the structure size and overall mass of the seeding device[9]. The diameter of the type hole and suction hole is related to the three-dimensional size of rice seeds, which can be calculated according to the following equation:

$$D_a = \left(\sqrt{\frac{b^2 + 3a^2}{3}} + a \right) \tag{1}$$

$$D_b = (0.64 \sim 0.66)b \tag{2}$$

where, D_a is the minimum hole diameter for holding three rice seeds, mm; D_b indicates the diameter of suction hole, mm; a stands for long axis of rice seeds, mm; and b is the short axis of rice seeds, mm.

Conventional Huanghuazhan rice seeds were selected for the experiment, and the long axis×short axis×thickness was about 9.41 mm×2.31 mm×1.90 mm[10]. The minimum hole diameter was calculated with Equation (1) as 4.22 mm. Considering the fluidity of rice seeds in the seed filling chamber, the optimal hole diameter range was 4-6 mm. According to Equation (2), the diameter of the suction hole ranged from 1.48 to 1.52 mm.

The structure of the seeding plate is shown in Figure 4. Suction holes on the seeding plate are arranged next to the type holes on the side closer to the center of the seeding plate, and the diameter of the seeding plate is determined by the size and number of type holes, which can be expressed as

$$K = \frac{\pi D v_m}{(1-c) I_z v_d} \tag{3}$$

$$v_d = \pi D n \tag{4}$$

where, K is the number of type holes on one single side; D represents the seeding plate diameter, mm; v_m is machine operating speed, m/s; c stands for the ground wheel sliding rate, %; I_z is the inter-seed distance, mm; v_d represents linear velocity of the seeding plate, m/s; n indicates the rotation speed of the seeding plate, r/min.

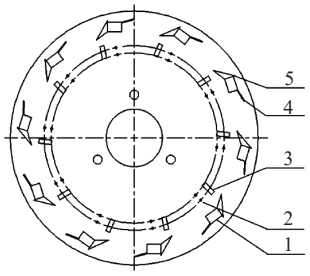

1. Type hole; 2. Suction hole; 3. Strip stirring teeth; 4. Type hole stirring plate; 5. Type hole tail plate.

Figure 4 Structural diagram of the seeding plate

According to the agronomic requirements, the seeding distance of Huanghuazhan rice seed is generally 150 mm; the designed rotation speed of the seeding plate is 20 r/min; the sliding rate of the ground wheel is 10%; and the forward speed of the machine is 1.2 km/h. The number of type holes in a single side of the seeding plate was calculated by Equations (3) and (4) as 7.4. To ensure the working efficiency, the number of type holes in a single side is set as 10. The diameter of the seeding plate is designed to be 192 mm. In order to ensure the strength of the seeding plate, the thickness is designed to be 2 mm.

To ensure seeding quality, each type hole should accommodate 3 seeds. The major axis dimension of a single seed is 9.41 mm. The spacing between type holes should be greater than 30 mm. There are 10 type holes in the seeding plate, and the circumference of the circular distribution of type holes should be greater than 390 mm. The formula for calculating the radius (R_a) of the circular distribution of type holes is as follows:

$$R_a \geq \frac{K(L+a)}{2\pi} \tag{5}$$

where, K is the number of type holes; L is the spacing between type holes, mm; and a is the major axis dimension of the seed, mm.

According to Equation (5), the calculated radius (R_a) of the circular distribution of type holes is greater than 62.1 mm. Considering the uniform distribution of type holes on the seeding plate, the radius of the circular distribution of type holes is approximately 62.1-77.0 mm. Subsequent Section 4.2.1 will continue to analyze the impact of the radius of the circular distribution of type holes on seeding performance.

Meeting the design requirements of a combined adjustable seeder, the seeding plate needs to simultaneously arrange type holes and suction holes. Designing double rows of suction holes to simultaneously adsorb rice seeds, the quantity of suction holes in a single row is consistent with the number of type holes, set at 10. When the spacing between double rows of suction holes is too small, disturbances between the two suction holes may occur, hindering seeding and carrying of seeds. When the spacing between suction holes is too large, the seeding into the hole becomes inconsistent. Considering that the tail of the stirring plate does not affect the adhesion of rice seeds to the suction holes, the radius of the far suction hole is set at 62 mm. As analyzed earlier, the diameter of the suction hole is 1.48-1.52 mm. The minimum spacing between two rows of suction holes is 3.04 mm to ensure smooth adhesion of seeds. The maximum spacing between suction holes should be less than the major axis dimension of the rice seed, which is 9.41 mm. Therefore, the range of suction hole spacing is 3.04-9.41 mm. Subsequent Section 4.2.4 will further analyze the impact of suction hole spacing on pressure.

3.2 Analysis of the seeding process

By analyzing the process of seed filling, seed protecting, and seed casting of the rice seed metering device, its kinematic and dynamic models were established, and the key parameters affecting its performance were determined, laying a theoretical basis for the optimized design of the rice seed metering device.

3.2.1 Seed filling process

1) Seed filling process of the type hole

In the seed filling chamber, the type hole stirring plate continuously stirs the seeds along with the rotation of the seeding plate, and seeds are filled into the type hole under the action of their own gravity, the supporting and friction force of the stirring plate, as well as the supporting and friction force between seeds. Single seeds filled into the type hole in the filling chamber were taken as research objects, and the rice seed was simplified into an ellipsoid shape[11].

The relative motion coordinate system was established, respectively. The relative coordinate system diagram of rice seed and seed disc relative to mold hole is shown in Figure 5. According to the positions of the rice seed centroid upon contact with the type hole stirring plate, the centroid was divided into three different positions on the inside, the tip, and the outside of the seed stirring plate, and force analysis of rice seeds was carried out, respectively. The trajectory equation of the origin of the second coordinate system in the first coordinate system is as follows:

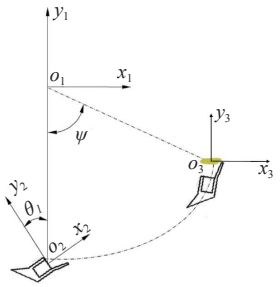

Note: o_1 is the center of the seeding plate and the origin of the first coordinate system. The ground horizontal direction is the x-axis, and the gravity direction is the y-axis. o_2 is the origin of the second coordinate system. The axial direction of the I-hole is the x-axis and the radial direction is the y-axis. The centroid of the rice seed o_3 is the origin of the third coordinate system. The long axis of rice seed is the x-axis and the short axis is the y-axis.

Figure 5 Schematic diagram of the coordinate system of rice seeds and type holes relative to the seeding plate

$$\begin{cases} x_2 = l\cos\theta \\ y_2 = l\sin\theta \\ \theta = \omega t \end{cases} \tag{6}$$

where, l is the distance from the origin of the second coordinate system to the center of the origin of the first coordinate system, mm; θ_1 is the angle (°) between the axis of line o_1o_2 and y_2; and ω represents uniform rotation angular velocity of the type hole around the seeding plate, rad/s.

When the centroid of rice seeds is outside the seed stirring plate of the type hole as shown in Figure 6a, the transverse profile of rice seeds satisfies the elliptic equation.

$$\frac{x^2}{a^2} + \frac{y^2}{b^2} = 1 \tag{7}$$

The contact point between the type hole stirring plate and rice seed is defined as C, whose coordinate of point is:

$$C\left(-s, \sqrt{b^2 - b^2\left(\frac{s}{a}\right)^2}\right),\ 0 < s < a \tag{8}$$

The linear equation of resultant force of rice seed on the outside of the type hole stirring plate was established as:

$$y = \cot\theta x \tag{9}$$

The moment arm equation of the line between C and the resultant force is:

$$l_1 = \left| b\cos\theta\sqrt{1 - \frac{s^2}{a^2}} - s\sin\theta \right| \tag{10}$$

The seed moment equation is:

$$M = \vec{F}_1 \cdot L = F_1 l_1 \tag{11}$$

Equations (10) and (11) are combined to obtain the moment of rice seed on the outside of the seed stirring plate in the type hole.

$$M = F_1\left| b\cos\theta\sqrt{1 - \frac{s^2}{a^2}} - s\sin\theta \right| \tag{12}$$

where, s is the distance between the tip of type hole seed stirring plate and the centroid of rice seed in the third coordinate system, mm; θ is the angle (°) that the type hole rotates in Δt time in the second coordinate system; l_1 represents the distance between the contact point of type hole seed stirring plate and rice seed from F_1, mm; F_1 is the supporting force of rice seeds to a rice seed in the filling chamber, N; F_S represents the friction force of type hole seed stirring plate on rice seeds, N; G is the gravity of rice seeds, N.

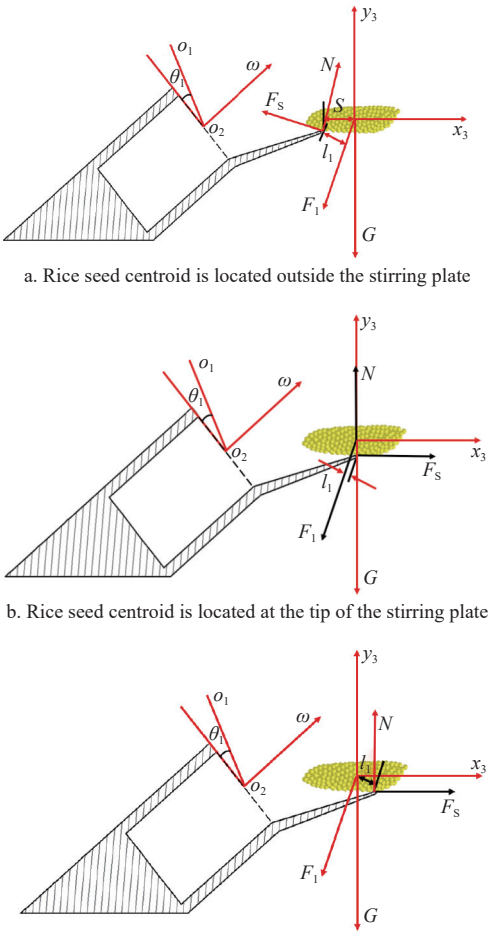

a. Rice seed centroid is located outside the stirring plate

b. Rice seed centroid is located at the tip of the stirring plate

c. Rice seed centroid is located inside the stirring plate

Figure 6 Three positions of rice seed centroid relative to the type hole

When the centroid of rice seed is located at the tip of the stirring plate as shown in Figure 6b, the moment arm of the supporting force F_1 of the rice seeds in the filling chamber on a rice seed is:

$$l_1 = b\sin\left(\theta + \delta - \frac{\pi}{2}\right) \tag{13}$$

The moment equation was established for the rice seed at the tip of the stirring plate as:

$$M = F_1 b\sin\left(\theta + \partial - \frac{\pi}{2}\right) \tag{14}$$

where, δ is the included angle between the supporting force F_1 of rice seeds on a rice seed in the filling chamber and the gravity of rice seed, (°).

When the centroid of rice seed is located inside the stirring plate as shown in Figure 6c, the state is opposite to that when the centroid of rice seed is located outside the stirring plate, and the torque equation is:

$$M = -F_1\left| b\cos\theta\sqrt{1 - \frac{s^2}{a^2}} - s\sin\theta \right| \tag{15}$$

According to the analysis of the position relation between the rice seed centroid and the type hole, there are the following three situations. In the first case, when the rice seed is outside the stirring plate, the torque M is positively correlated with the supporting force of rice seeds in the filling chamber on the rice seed, and the

resultant force on the rice seed points to the third quadrant of the third coordinate system, and the seeds roll out of the type hole and cannot fill the hole. In the second case, when the rice seed centroid is inside the stirring plate, under the action of gravity of the rice seed itself and the supporting force of the stirring plate, the resultant force of rice seed points to the type hole, and the filling success rate is high. In the third case, the filling success rate of rice seeds depends on the horizontal distance between the tip of the stirring plate and the rice seed centroid. The length and angle of the stirring plate are key factors affecting the filling success rate of rice seeds. As can be seen from Equation (14), the supporting force of rice seeds on a rice seed first increases and then decreases with increasing angle of the stirring plate. The radius of the short axis of the rice seed is b = 1.115 mm; when the tilt angle of the stirring plate plane and the x-axis of the first coordinate system is 30°, δ = 60°; the angle of the end plane of the stirring plate and the second coordinate system θ = 120°; $\sin(\theta+\delta-\pi/2)$ approaches 0, the moment arm reaches the minimum value, and the support force of rice seeds on a rice seed reaches the maximum value.

2) Suction and seed filling process

In the suction hole, a negative-pressure chamber is formed by connecting the chamber to a fan. Rice seeds are sucked to the suction hole by negative pressure, and the seed filling process is completed by overcoming the gravity of the rice seed itself, friction between the rice seed and the seeding plate, and the reactive force of the seeding plate[12]. The suction force provided by the negative-pressure air chamber is the key factor affecting the pneumatic seeding. Due to the small size of rice seeds, the influence of the surrounding suction holes on the sucked rice seed can be ignored, and a shell is installed on both sides of the seeding plate, and the air resistance can be ignored[13]. The force model can be established as shown in Figure 7.

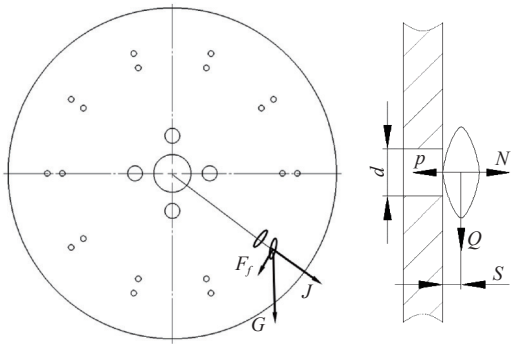

Figure 7 Seed suction process of the seeding plate

The equation of resultant force Q on rice seed is:

$$Q = G + F_f + J \tag{16}$$

The torque balance equation that needs to be satisfied to realize the filling of rice seeds by the suction hole is:

$$(P - N)\frac{d}{2} = QS \tag{17}$$

After sorting out Equation (16), Equation (17) can be obtained as:

$$P\frac{d}{2} = QS + N\frac{d}{2} \tag{18}$$

The sucked rice seeds rotate with the seeding plate, which needs to satisfy:

$$P\frac{d}{2} > QS \tag{19}$$

In order to ensure that the rice seed does not fall off from the suction hole, the negative- pressure air chamber must meet the following critical vacuum degree:

$$p = \frac{\frac{8S}{\pi d^3}\sqrt{G^2 + J^2 + 2GJ\cos\chi + F_f^2}}{2F_f\sqrt{G^2 + J^2 + 2GJ\cos\chi}\cos\sigma} \tag{20}$$

Since the direction of gravity, friction, and inertia force of rice seed is the same, $\cos\chi$=$\cos\sigma$=1, λ = (6~10) $\tan\theta$ is substituted into Equation (20) to obtain the maximum critical vacuum degree p provided by the negative-pressure chamber:

$$p = \frac{8K_1K_2SG}{\pi d^3}\left(1 + \frac{n^2}{Gr} + \lambda\right) \tag{21}$$

where, F_f is the friction force between rice seeds and seeding plate, N; J represents the inertia force of rice seeds circling with the seeding plate, N; P indicates the suction force of negative- pressure cavity on rice seeds, N; N stands for the supporting force of the seeding plate on rice seeds, N; d is the diameter of the suction hole, mm; S represents the distance between rice seed centroid and end plane of the seeding plate, mm; χ is the angle between gravity and inertia force J of rice seed, (°); σ is the angle between the resultant force and the friction force of rice F_f, (°); λ is the friction resistance coefficient of rice seeds and seeding plate, 0.16; r is the distance between seeding position and seeding plate axis, mm; K_1 represents the reliability coefficient of field stability; and K_2 is the reliability coefficient of suction.

In order to ensure the suction of rice seeds by the suction hole, the pressure of the negative- pressure chamber should be greater than the maximum critical vacuum degree p. It can be seen from Equation (21) that the maximum critical vacuum degree p is related to the diameter of the suction hole d, and decreases with increasing diameter of the suction hole. K_1 and K_2 are generally 1.8-2.2 and 1.6-2.0, respectively. The vacuum degree of reference pneumatic rice seeding plate is generally 2.0-3.6 kPa, and the distance between the rice seed centroid and the end plane of the seeding plate is half of the thickness of rice seeds. Therefore, S is set as 0.95 mm; the 1000-grain weight of Huanghuazhan rice is about 18-34 g; the gravity G of single rice seeds is about 0.018-0.034 g. A higher p represents that the diameter of the suction hole should be smaller. The rotation speed of the seeding plate is 20 r/min. The distance between the seed position and the seeding plate center is 80 mm, and the suction hole diameter is about 1.5 mm when the minimum vacuum degree p of the seeding plate is 2.0 kPa and the maximum grain gravity is 0.034 g.

3.2.2 Analysis of the seed protection process

According to the working principle, the device enters the seed protection stage when the type hole and suction hole complete seed filling and rotate to contact with their seed clearing brush, respectively[14]. The PA6 brush of 0.1 mm was used in both the type hole cleaning brush and the suction hole cleaning brush. The pre-test found that the PA6 type cleaning brush would not be too soft to affect the seed cleaning effect, nor would it damage the rice seeds. Rice seeds sucked by the suction hole always keep contact with the seeding plate during the whole protection stage, but when rotating with the seeding plate, rice seeds in the type hole will break away from the type hole due to the disruption of the force balance, as shown in Figure 8. When the rice seed is in position 1, the supporting force of the type hole on the rice seed overcomes the friction between the rice seed and type hole, making the rice seed completely enter the type hole and move smoothly. Position 2 is the position of type hole at the top of the seeding plate. Force analysis was carried out on the rice seeds at position 2, as shown in Figure 9.

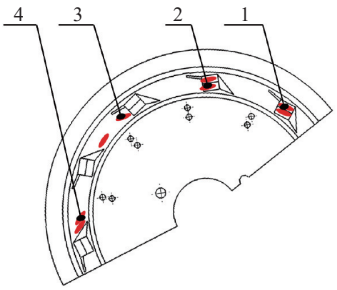

1. Rice seed is located inside the type hole; 2. Rice seed is at the critical point of stress equilibrium; 3. Rice seed is deposited at the stirring plate end of the front type hole; 4. Rice seed is deposited to the end of the type hole.

Figure 8 Schematic diagram of seed protection process

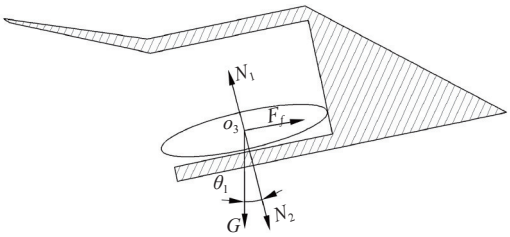

Figure 9 Force analysis of rice seeds in the type hole

The motion equation of rice seeds was established as:

$$G\sin(\theta_1+\theta)-\mu N_2-\mu G\cos(\theta_1+\theta)=ma \tag{22}$$

where, μ is the friction coefficient between rice seeds and type hole; N_2 represents the pressure on target rice seeds by rice seeds in the type hole, N; and a is the instantaneous acceleration at which the seed starts to move, m/s^2.

In position 2 of Figure 8, the gravity component force of the rice seed gradually increases, and the pressure and friction resistance of rice seeds in the type hole on the target rice seed gradually decreases. When the friction force of the rice seed cannot overcome the influence of its gravity, the force balance of the rice seed is broken. When the seeding plate continues to rotate to position 3 in Figure 8, the component force provided by the gravity of rice seed is greater than the friction force between the rice seed and type hole, and the seeds break away from the type hole and gradually fall down until they accumulate at the end of the front type hole, and reach a relatively stable state under the supporting force of the stirring plate end of the previous type hole.

3.2.3 Analysis of the seeding process

At the seeding stage of the device, it is necessary to gather the rice seeds entering the type hole and suction hole in the same place. The seeding process is shown in Figure 10. Rice seeds sucked by the suction hole enter the positive-pressure chamber and fall to the seed protection groove under the action of their own gravity and positive pressure, and then fall to the end of the front type hole together with rice seeds in the type hole, completing the mechanical and pneumatic seed gathering process.

For rice seeds sucked by the suction hole, the height of falling into the seed protection groove is h; the time from falling to reach the seed protection groove under the action of gravity is t; the rotation angle of the suction hole is γ; the angle between the suction hole and the type hole stirring plate is β. Then, there is:

$$\begin{cases} h=v_0t+\dfrac{gt^2}{2} \\ \gamma=\dfrac{nt}{60}\times 360^\circ \\ \beta=\dfrac{\pi}{2}-\alpha-\gamma \end{cases} \tag{23}$$

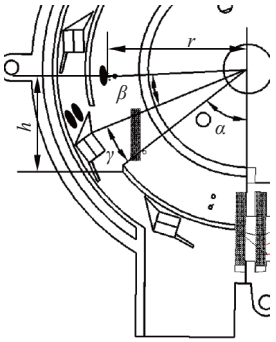

Figure 10 Schematic diagram of the seeding process

$$\beta=\frac{\pi}{2}-\alpha-\frac{-v_0n+n\sqrt{v_0^2+2hg}}{g}\times 60^\circ \tag{24}$$

where, n is the rotation speed of the seeding plate, r/min.

The initial rotation velocity of rice seeds sucked by the suction hole with the seeding plate is:

$$v_0=\omega r \tag{25}$$

The following kinematic equation can be established for the rice seed fallen from the seed protection groove:

$$\begin{cases} x=v_0\cos\theta t \\ y=v_0\sin\theta t+\dfrac{1}{2}gt^2 \end{cases} \tag{26}$$

Equations (24)-(26) are combined to obtain the fitting equation of the motion trajectory of rice seed:

$$y=1333.16x^2+0.7x \tag{27}$$

where, x is horizontal displacement of rice seeds, mm; and y indicates the vertical displacement of rice seeds, mm.

Kinematic analysis of the seeding process indicates that when the structural parameters of the seeding plate are fixed, the motion track of rice seeds is related to the rotation speed of the seeding plate. The motion distance of the rice seed axis center from the seeding mouth of seed protection groove to the end face of the seeding plate is designed as r = 80 mm, and the rotation speed of the seeding plate is designed to be n = 20 r/min. The rotational angular velocity of the seeding plate can be obtained from Equation (25) as ω = 18.84 rad/s, indicating that when the seeding plate is rotated 18.84° in one second, rice seeds sucked by the suction hole can just fall to converge with rice seeds from the type hole. Therefore, the rotation angle of the suction hole γ is set at 18.84° and then substituted into Equation (23) to obtain t = 0.95 s < 1 s, indicating that the rice seed separation meets the requirements of the seeding operation of the rice seeds sucked by the suction hole.

4 Performance test and parameter optimization based on EDEM-Fluent coupling simulation

Discrete element method (DEM) and Finite element method have been widely applied in agricultural engineering in recent years[15,16]. In order to verify the seeding performance of the designed rice seed metering device, EDEM-Fluent coupling simulation was used to optimize the structural parameters of the type hole, suction hole, and stirring plate[17].

4.1 Establishment of the simulation model

4.1.1 Discrete element model

The discrete element model for the rice seed metering device is shown in Figure 11. The air chamber shell is set as ABS material, and the seeding plate is set as aluminum alloy, which is consistent

with the actual processing material of seed metering devices. The rice variety is Huanghuazhan, with a size of long axis × short axis × thickness of about 9.41 mm×2.31 mm×1.90 mm. With the help of the application programming API interface provided by EDEM, global variables were set; the coordinates and particle size of rice seed contour filling ball particles were extracted respectively on the post-processing interface; and rice seed particle factory was written. Based on the Hertz-Mindlin with bonding contact model, a rice seed discrete element model was constructed as shown in Figure 12. By referring to relevant literature, rice seed intrinsic parameters and contact parameters are obtained and listed in Table 1[18-20].

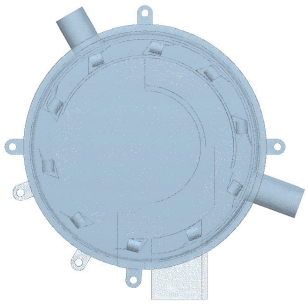

Figure 11 Discrete element model of the rice seed metering device

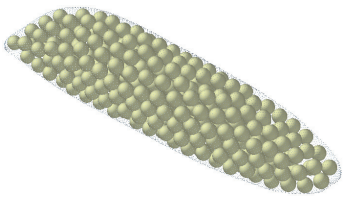

Figure 12 Discrete element model of rice seeds

Table 1 Basic simulation parameters of EDEM

Items	Property	Value
Rice seed	Poisson's ratio	0.3
	Shear elasticity/Pa	1.1×10^{7}
	Density/kg·m^{-3}	1130
Shell	Poisson's ratio	0.3
	Shear elasticity/Pa	7×10^{10}
	Density/kg·m^{-3}	7850
Rice-Rice	Elastic recovery coefficient	0.3
	Coefficient of sliding friction	0.56
	Coefficient of rolling friction	0.01
Rice-Shell	Elastic recovery coefficient	0.5
	Coefficient of rolling friction	0.5
	Elastic recovery coefficient	0.01

4.1.2 EDEM-Fluent coupling boundary conditions

The Fluent software was used to carry out the simulation test, assuming incompressible metering chamber air and atmospheric pressure of 1.01×10^{5} Pa; the metering device inside was kept at a constant temperature of 25°C; turbulence k-ε model was chosen; transient calculation was carried out; the grid type was set to Mesh Motion; and simple algorithm and the residual coefficient of 1.0×10^{-4} was used. According to the requirements of EDEM-Fluent coupling simulation, the time step of EDEM was set to be 100 times of the time step of Fluent in order to maintain the stability of calculation.

4.2 Performance simulation and analysis

4.2.1 Influence of type hole distribution on seed filling performance

In order to explore the effect of type hole distribution on the seed filling performance, by taking the radius of type hole center distribution cycle as a factor and referring to the standard of NY/T 987-2006, the seeding of the hybrid rice was qualified by precise seeding (2±1) seeds/hole, missed seeding (0 seeds/hole), qualified seeding (1-3 seeds/hole), and repeated seeding (≥ 4 seeds/hole). A single-factor simulation test was carried out with qualification rate A, missing rate M, and repeating rate D as the evaluation indices of the seed filling performance.

$$A=\frac{N_0}{N_f}\times100\% \tag{28}$$

$$M=\frac{N_1}{N_f}\times100\% \tag{29}$$

$$D=\frac{N_a}{N_f}\times100\% \tag{30}$$

where, N_0 indicates that the number of seeds in the type hole is 1-3; N_1 means that the number of seeds in the type hole is 0; N_a represents that the number of seeds in the type hole is 4 or above.

According to the theoretical analysis in Section 3.1, the calculated radius for the circular distribution of type holes is approximately 62.1-77.0 mm. Therefore, in Section 4.2.1, the radius of the circular distribution of type holes is set at 65 mm, 70 mm, and 75 mm for a three-level single-factor simulation experiment on the performance of type hole distribution.

As listed in Table 2, with increasing radius of the distribution circle of the type hole center, the qualified rate shows no significant change, and the missing rate shows a first decreasing and then increasing trend. A larger radius of the distribution circle of the type hole represents a larger seed filling travel distance and a larger number of seeds in contact, thereby decreasing the missing rate. The radius of the distribution circle has a significant effect on the missing rate.

Table 2 Test results of type hole distribution

Radius of the distribution circle of type holes/mm	Qualified rate/%	Missing rate/%	Repeating rate/%
65	68.00	16.00	16.00
70	68.19	13.63	18.19
75	63.15	21.05	15.79

4.2.2 Influence of seed stirring plate on seed stirring performance

Theoretically, the speed of seeds at a certain time is not lower than 4.9 mm/s, indicating that the rice seed complies with the seed mobility characteristics[21,22]. In order to explore the effect of stirring plate on the seed filling performance, it is assumed that the distance of rice seed centroid moving within 1 s is more than half of the length of the rice seed itself, and the stirring ratio N is taken as the evaluation index of seed stirring to carry out a single-factor simulation test of non-stirring plate and stirring plate. The test results are listed in Table 3.

Table 3 Test results of influence of seed stirring plate

Factor	Qualified rate/%	Missing rate/%	Repeating rate/%	Stirring ratio/%
No stirring plate type hole	63.15	21.05	15.79	55.16
Type hole with stirring plate	71.42	9.52	19.04	57.13

$$N=\frac{n_1}{n_j} \tag{31}$$

where, n_1 is the number of seeds with velocity greater than 4.9 mm/s at a certain time in the filling chamber, and n_j represents the number of rice seeds in the filling chamber at any given time.

As shown in Table 3, the type hole with a stirring plate has a much greater stirring ratio than the type hole without a stirring plate, and as a result has a significantly higher qualified rate and lower missing rate. This indicates that the seed stirring plate has a good stirring effect on rice seeds, and seeds with different postures can enter the type hole along the stirring plate[23]. In order to further explore the stirring performance of the seed stirring plate on rice seeds, the rice seeds in the filling chamber were marked with five different colors and recorded as the initial positions of different rice seeds, as shown in Figure 13a. The test results after 4 s of stirring are shown in Figure 13b, which clearly shows a good stirring effect on the seeds.

In order to verify whether the seeds will be damaged by the disturbance of the population, the filling of seed by the type hole, the protection of the seed and the discharge of the seed during the mechanical seeding operation, stress analysis of the rice seed is needed. The single rice seed that successfully bagged into the type hole and completed the whole seeding operation in the simulation test was selected. The stress change curve of rice seed over time was shown in Figure 14. The analysis showed that the stress on rice seed during seed filling was greater than that during seed protection and seeding, and the maximum force on rice seed was 0.06 N, far less than the theoretical seed damage value of 3.2 N[24]. Therefore, the seed dispenser does not hurt seed when the mechanical operation is adopted.

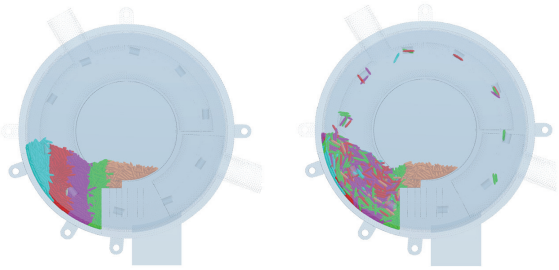

a. Initial positions of rice seeds in the seed filling chamber b. Positions of rice seeds after 4 s of stirring

Figure 13 Effect of seed stirring

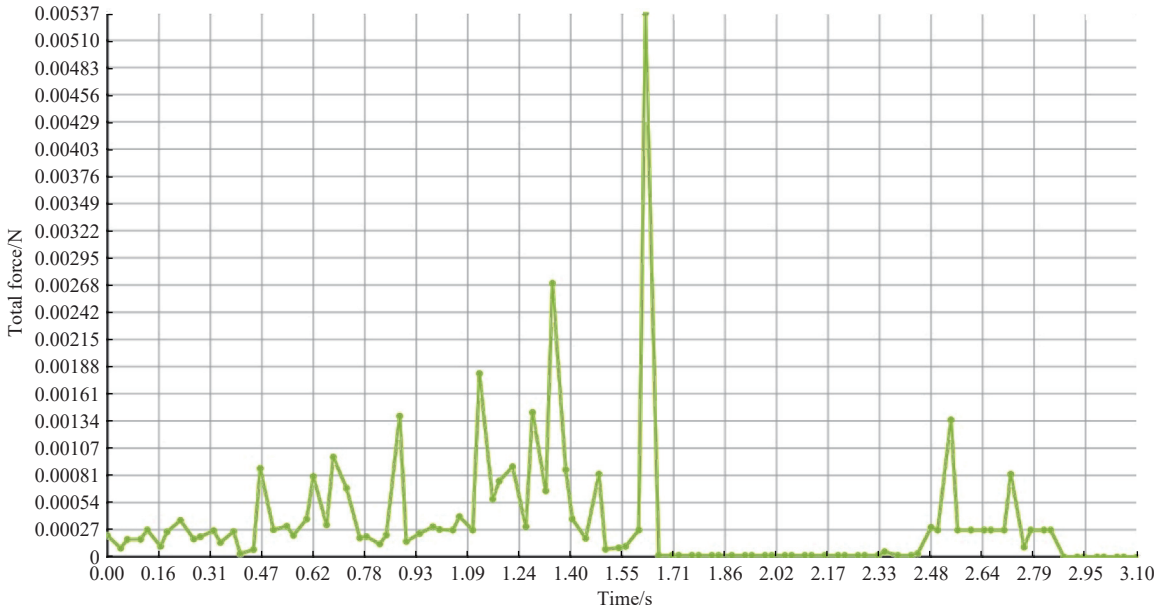

Figure 14 Force on rice seeds in the seed discharger over time

4.2.3 Response surface optimization test of the type hole and stirring plate

1) Experimental design

The type hole diameter and the length and tilt angle of the stirring plate are important factors affecting the qualified rate of filling. With the diameter of the type hole x_1, the length of the stirring plate x_2, and the tilt angle x_3 as the test factors, and the qualified rate as the index, a simulation test of three factors and three levels was carried out. The factor levels are listed in Table 4.

Table 4 Factor levels for the simulation test

Level	Factor		
	Type hole diameter x_1/mm	Stirring plate length x_2/mm	Stirring plate tilt angle x_3/(°)
–1	4	5	10
0	5	7	20
1	6	9	30

According to the theoretical analysis in Section 3.1, the optimization range of type hole diameter should be 4-6 mm. Therefore, simulation tests were carried out with the type hole diameters of 4 mm, 5 mm, and 6 mm.

According to the theoretical analysis in Section 3.2.1, when the centroid of rice seed is in the inner side of the seed mixing plate with type hole, the long axis of rice seed is 9.410 mm, the tip of the seed mixing plate is 4.705 mm away from the seed centroid of rice seed, and the length of the seed mixing plate should be larger than 4.705 mm to ensure that rice seed can fit into the type hole. If the length of the mixing board is too long, it will prolong the time for rice seed sac to enter the mold hole, which is not conducive to seed filling. The long axis of rice seed is taken as the maximum length of the mixing board, and the length range of the mixing board is 4.705 mm to 9.410 mm. Therefore, simulation tests were carried out with the lengths of 4 mixing plates of 5 mm, 7 mm, and 9 mm.

The length and angle of the type hole stirring plate are the key factors affecting the success rate of filling. With the increase of the angle of the stirring plate, the supporting force of the population on the rice seed increases first and then decreases. The radius of the short axis of the rice seed b=1.115 mm. When the angle of the

stirring plate plane and the first coordinate system x- axis square is 30°, δ=60°, the angle of the end face of the stirring plate and the second coordinate system θ=120°, $\sin(\theta+\delta-\pi/2)$ approaches 0. When the lever reaches the minimum value, the supporting force of the population to the rice seed reaches the maximum value. Therefore, simulation tests were carried out at 10°, 20°, and 30° for the tilt angle of the stirring plate.

2) Results and analysis

The test results are listed in Table 5. The Design-Expert software was used to analyze the variance of the results (Table 6).

Table 5 Test results

Test	Level of factor			Qualified rate/%
	x_1	x_2	x_3	
1	–1	–1	1	73.91
2	–1	0	–1	65.21
3	–1	0	1	58.33
4	–1	1	0	66.67
5	0	–1	–1	71.42
6	0	–1	1	69.56
7	0	0	0	61.90
8	0	0	0	66.67
9	0	0	0	60.00
10	0	0	0	62.00
11	0	0	0	58.50
12	0	1	–1	61.90
13	0	1	1	40.00
14	1	–1	0	35.00
15	1	0	–1	44.00
16	1	0	1	44.00
17	1	1	0	35.00

Table 6 Analysis of test variance

Source	Sum of squares	Degree of freedom	Mean square	F	p
Model	2267.90	9	251.99	8.60	0.0049
x_1	1160.42	1	1160.42	39.59	0.0004
x_2	190.03	1	190.03	6.48	0.0383
x_3	197.41	1	197.41	6.74	0.0357
x_1x_2	12.29	1	12.29	0.4191	0.5380
x_1x_3	11.83	1	11.83	0.4037	0.5454
x_2x_3	212.28	1	212.28	7.24	0.0310
x_1^2	474.05	1	474.05	16.17	0.0050
x_2^2	9.46	1	9.46	0.3229	0.5876
x_3^2	11.91	1	11.91	0.4063	0.5441
Residual	205.18	5	29.31		
Lack of fit	167.28	3	55.76		
Pure error	37.90	2	9.47		
Cor total	2438.21	16			

Analysis of variance results show that regression coefficient R^2=0.9170, model p<0.01, and the regression coefficient is extremely significant. The three factors influencing the qualified rate are type hole diameter, stirring plate angle, and stirring plate length. The interaction between the stirring plate length and stirring plate angle had a significant effect on the qualified rate of seed filling, and the regression equation was obtained as

$$A = 61.81 - 12.04x_1 - 44.81x_2 - 44.97x_3 + 1.75x_1x_2 + 1.72x_1x_3 - 7.29x_2x_3 - 10.61x_1^2 + 1.5x_2^2 + 1.68x_3^2 \quad (32)$$

The response surface of the interaction between the stirring plate length and tilt angle is shown in Figure 15. When the diameter of the type hole is fixed, the qualified rate of filling decreases with increasing tilt angle of the stirring plate. The qualified rate of seed filling also decreases with increasing length of the stirring plate. Multi-objective optimization was carried out with the highest qualified rate as the optimization objective. The results show that at the type hole diameter of 6 mm, stirring plate length of 5 mm, and stirring plate tilt angle of 10°, the best performance could be obtained, with a qualified rate of 71.42%.

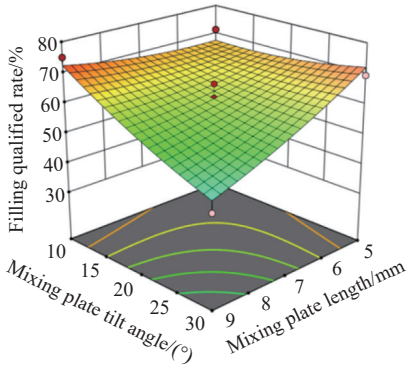

Figure 15 Response surface of the stirring plate tilt angle and length for the qualified rate

4.2.4 Optimization of suction hole structure and parameters

1) Experimental design

The pressure and velocity at the outlet of the suction hole are key factors affecting the seed filling performance of the device. In order to explore the influence of the diameter and spacing of the suction hole on the pressure and velocity at the outlet of the suction hole in the rotating flow field[25], a two-factor and three-level test was carried out with the spacing and diameter of the suction hole as influencing factors and the average pressure in the center of the suction hole as the evaluation index. Factor levels are listed in Table 7.

Table 7 Test factor levels of the spacing and diameter of the suction hole

Level	Factor	
	Hole spacing x_4/mm	Hole diameter x_5/mm
1	4	1.3
2	6	1.5
3	8	1.7

According to the theoretical analysis in Section 3.1, the optimized range of suction hole spacing is 3.04-9.41 mm. Therefore, the simulation test was carried out with the suction hole spacings of 4 mm, 6 mm, and 8 mm.

Calculated in Section 3.2.1, the diameter of the suction hole ranges from 1.48 to 1.52 mm. Therefore, the suction hole diameters of 1.3 mm, 1.5 mm, and 1.7 mm were simulated.

2) Results and analysis

Figure 16 shows the cross-sectional diagram of the air chamber, suction hole, and filling chamber. The negative-pressure flow field of the air chamber and filling chamber is relatively stable. When the distance between two air chambers or two suction holes is too small, the pressure decreases to some extent, and the pressure from the suction hole along the air chamber to the filling chamber gradually decreases, while there is little difference in the vertical direction. The results of the two-factor test are listed in Table 8, and the variance analysis results are listed in Table 9.

Analysis of variance shows that the suction hole diameter has a significant effect on the average pressure in the center of the suction hole (p<0.05). The influence of suction hole diameter and spacing on the average pressure at the center of the suction hole is shown in Figure 17. When the negative pressure at the air inlet is –3600 Pa at a constant suction hole spacing, the average pressure at the center of the suction hole gradually decreases with increasing spacing of the suction hole. When the diameter of the suction hole is constant, the average pressure in the center of the suction hole first increases and then decreases with increasing diameter of the suction hole. When the distance between two adjacent suction holes is too small, there is disturbance between the two holes, whose influence gradually decreases with increasing spacing between the holes. When the spacing between two adjacent suction holes increases to 8 mm, it is not suitable for seeding anymore. To enhance the consistency of seeding, the spacing between adjacent suction holes should be reduced as much as possible. Finally, the suction hole diameter and the spacing are set as 1.5 mm and 6 mm.

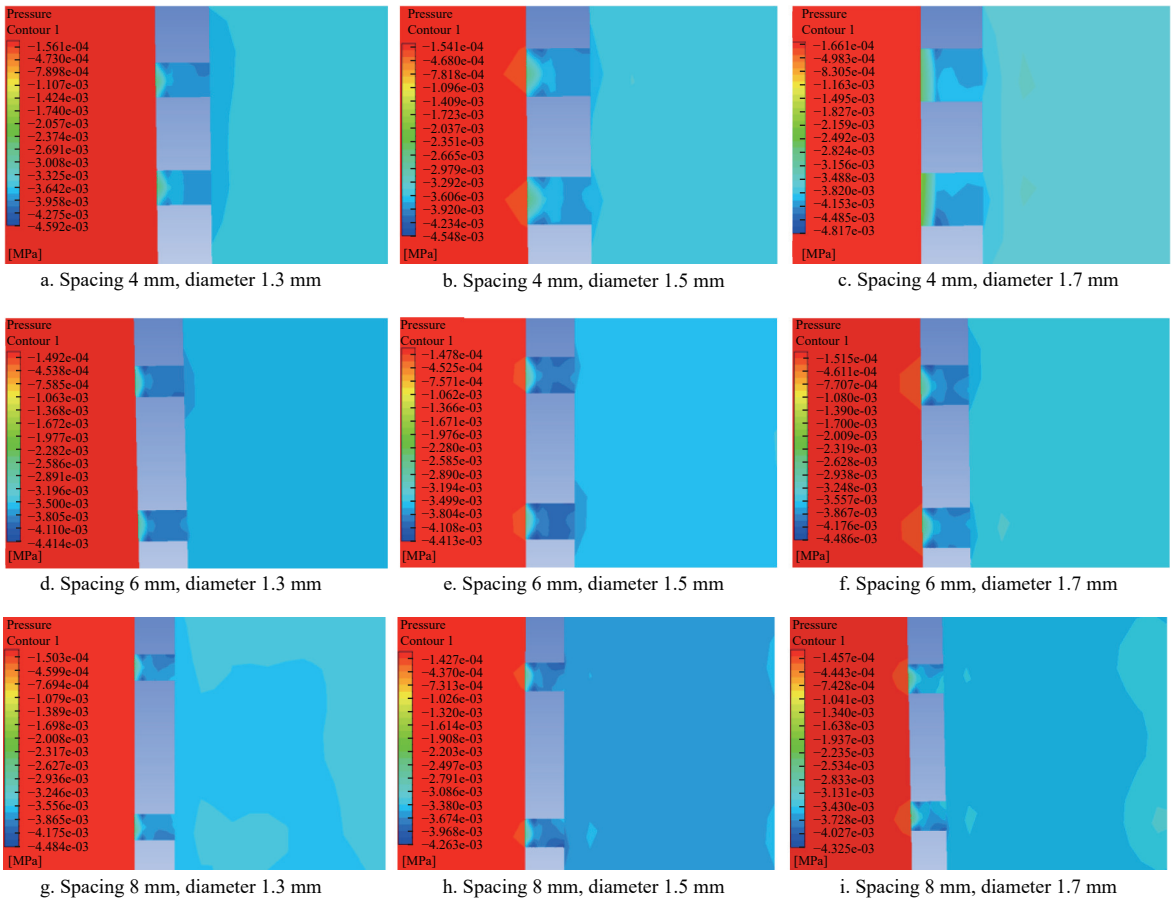

a. Spacing 4 mm, diameter 1.3 mm b. Spacing 4 mm, diameter 1.5 mm c. Spacing 4 mm, diameter 1.7 mm

d. Spacing 6 mm, diameter 1.3 mm e. Spacing 6 mm, diameter 1.5 mm f. Spacing 6 mm, diameter 1.7 mm

g. Spacing 8 mm, diameter 1.3 mm h. Spacing 8 mm, diameter 1.5 mm i. Spacing 8 mm, diameter 1.7 mm

Figure 16 Longitudinal section pressure cloud diagram of the suction hole

Table 8 Results of two-factor test

Test	Suction hole spacing/mm	Suction hole diameter/mm	Mean pressure/Pa
1	1	1	2676.00
2	1	2	2867.95
3	1	3	2800.00
4	2	1	2739.03
5	2	2	2824.56
6	2	3	2726.68
7	3	1	2329.25
8	3	2	2655.15
9	3	3	2569.43

Table 9 Analysis of variance of two-factor test results

Source of variation	Degree of freedom	F	$F_{0.05}(2,4)$	$F_{0.01}(2,4)$
Center distance of suction hole	2	4.486	6.94	18.00
Suction diameter	2	9.520*	6.94	18.00
Error	4			

Note: *indicates that the impact is significant.

4.2.5 Air chamber structure and parameter optimization

(1) Experimental design

The radius of air chamber is an important factor affecting the suction hole on the seeding plate[26]. In order to explore the influence of air chamber radius on the rotating flow field, the average pressures of the air chamber wall, suction hole inner center, suction hole outer center, and suction hole center were taken as evaluation indices.

The theoretical analysis and calculation in Section 3.1 shows that the diameter of the suction hole ranges from 1.48 to 1.52 mm, and the spacing of the suction hole ranges from 3.04 to 9.41 mm. The simulation analysis in Section 4.2.4 shows that the diameter of the suction hole on the seed discharge disc is 1.5 mm, the spacing of the suction hole is 6 mm, the spacing of the double suction hole is 9 mm, and the radius of the air chamber should be greater than 46 mm. Therefore, Section 4.2.5 carries out simulation tests with the chamber radii of 48 mm, 53 mm, and 58 mm.

(2) Results and analysis

Negative-pressure air chamber pressure and velocity cloud diagram is shown in Figure 18. When the spacing between the two adjacent suction holes, the radius of the air chamber, and the distance of the suction hole to the air chamber inner and outer ring remain unchanged, the change in the radius of the negative-pressure air chamber will affect the radius of the distribution circle of suction

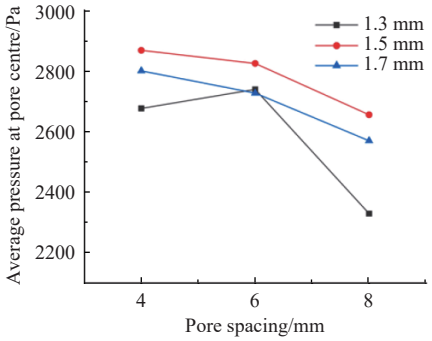

a. Different suction hole spacing

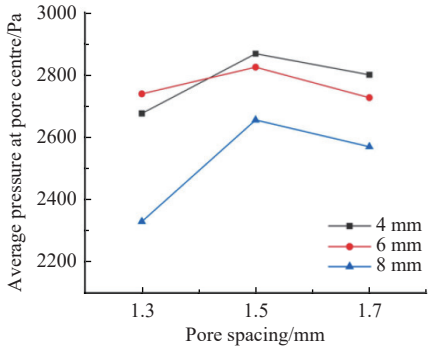

b. Different suction hole diameters

Figure 17 Effects of different suction hole spacing and diameters on the pressure in the center of the suction hole

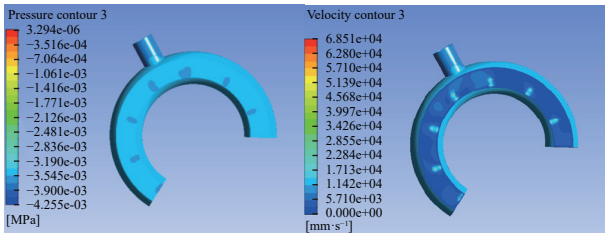

a. Inner and outer radius of negative pressure air chamber is 48 and 66 mm, respectively

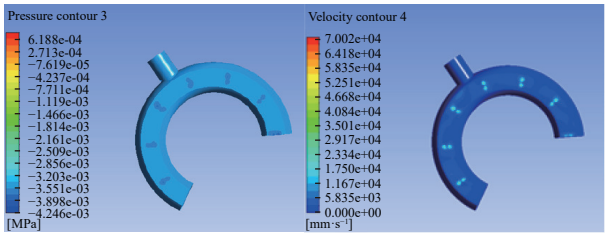

b. Inner and outer radius of negative pressure air chamber is 53 and 71 mm, respectively

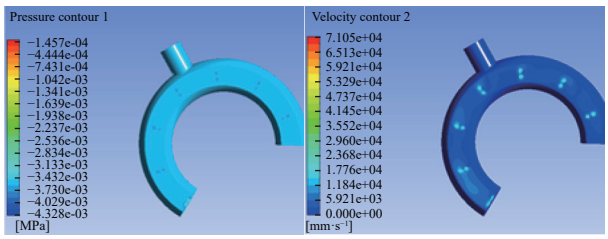

c. Inner and outer radius of negative pressure air chamber is 58 and 76 mm, respectively

Figure 18 Negative-pressure air chamber pressure and velocity cloud diagram

hole centers. As shown in Table 10, the wall pressure of the gas chamber flow field is relatively stable, and the pressure near the air chamber flow field in touch with the suction hole slightly decreases. With increasing radius of the air chamber, the pressure of flow field on the air chamber wall shows no obvious change. The outer center of the suction hole has higher average pressure than the inner center. When the chamber radius is 62 mm, there will be small differences in average pressure between the inner and outer suction hole centers, and the average pressure of the suction hole center is higher than the inner and outer pressure. Therefore, the chamber radius was determined to be 62 mm.

Table 10 Results for different air chamber diameters

Air chamber radius/mm	Average pressure on gas chamber wall/Pa	Average pressure in the inner center of suction hole/Pa	Average pressure in the outer center of suction hole/Pa	Average pressure in the center of suction hole/Pa
58	–3541.65	2200.15	2879.38	2539.77
62	–3527.87	2738.22	2772.09	2755.15
66	–3521.82	2578.12	2720.77	2619.44

5 Bench experiment and field experiment

On the basis of the simulation experiment, a bench performance test and field test on the regulation ability of the device on seeding amount were carried out to further evaluate the working performance of the designed rice seed metering device.

5.1 Bench experiment

5.1.1 Evaluation index

According to the national standard GB-T 6973-2005, sowing of regular rice varieties at 0-2 seeds/hole is considered as missed sowing, 3-6 seeds/hole as qualified sowing, and ≥ 7 seeds/hole as repeated sowing. Three sets of tests were repeated, with each group being recorded 250 times. The bench performance test was carried out with qualified rate, missing rate, repeating rate, hole distance qualified rate, and cavitation rate as the test indices.

The occurrence frequency $P(i)$ of different numbers of seeds per hole in the seeding process was calculated, and the formulas of qualified rate A, missing rate M, and repeating rate D were calculated:

$$P(i)=\frac{\sum_{j=1}^{3}x_{ij}}{750},\ i=0,1,2,3,4,5\ldots;j=1,2,3 \tag{33}$$

$$A=\sum_{i=3}^{6}P(i),\ i=3,4,5,6 \tag{34}$$

$$M=\sum_{i=0}^{2}P(i),\ i=0,1,2 \tag{35}$$

$$D=\sum_{i=7}^{n}P(i),\ i\geq 7 \tag{36}$$

where, i is the number of seeds per hole and j is the number of tests.

The theoretical value of the hole distance is 150 mm, and the number of holes with distance ranging from 135 to 165 mm was recorded. The qualified rate of the hole distance η_1 was calculated by dividing the number of effective hole distances by the total number of holes.

$$\eta_1=\frac{k_1}{k-1} \tag{37}$$

In terms of the identification of established holes, if the rice seed(s) are distributed in a circle with a diameter of 50 mm, it is identified as a hole[27], and the formula of the hole formation rate is

given as:

$$\eta_2 = \frac{k_2}{k} \tag{38}$$

where, k_1 is the total number of effective hole distances, k_2 is the total number of identified holes, and k represents the total number of holes.

5.1.2 Experiment process

The experiment was carried out on the performance test bench of JPS-12 visual seeding apparatus (Heilongjiang Academy of Agricultural Machinery Engineering, China) in the College of Engineering, Huazhong Agricultural University. The test device is shown in Figure 19. The same rice variety of Huanghuazhan was selected for the experiment. After seed soaking and bud promotion, the water content was measured as 19.78%. The length×width×thickness of the Huanghuazhan rice seeds is approximately 9.41 mm×2.31 mm×1.90 mm. Before sowing, it is necessary to pre-germinate and stain the rice seeds to enhance their advantages, such as high germination rate, drought resistance, lodging resistance, and high yield. Germinated and colored rice seeds are shown in Figure 20. The seeding device was installed on the test platform, and the speed was controlled by a motor to ensure that the speed of the conveyor belt matched with that of the seeding shaft. A layer of hydraulic oil film was laid on the conveyor belt, and rice seeds falling on the oil film were detected by a computer[28]. A fan was utilized to create negative pressure within the negative-pressure chamber, while the positive-pressure chamber was in communication with the external air, enabling rice seeds to detach from the suction holes under the influence of gravity.

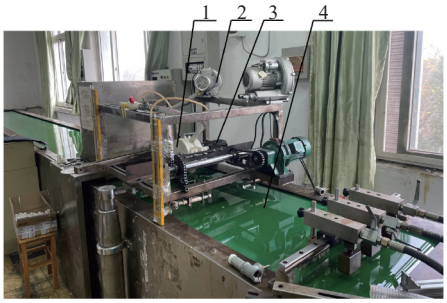

1. Seed metering device; 2. Fan; 3. Motor; 4. Conveyor belt

Figure 19 Performance test of the rice seed metering device

a. After germination b. After coloring

Figure 20 Rice seeds after germination and coloring

5.1.3 Performance analysis of the rice seed metering device

1) Influence of seeding plate speed on the seeding performance

To explore the influence of the rotation speed of the seeding plate on the performance of the device, a single-factor bench test of different rotation speeds of the seeding plate was carried out. The negative-pressure interface of the seeding plate was provided with a negative pressure of 3600 Pa, and the tilt angle between the suction hole and the end plate of the type hole was 24°. The test results are listed in Table 11.

As shown in Table 12, when the rotation speed of the seeding plate is 20-30 r/min, with increasing rotation speed of the seeding plate, excess rice seeds in the type hole cannot be brushed off by the clearing brush in time and fall into the seed protection groove, resulting in a higher repeating rate and a lower qualified rate. The cavitation rate of the device decreases gradually with increasing rotation speed of the seeding plate. A faster seeding plate rotation speed would result in a greater initial velocity of rice seeds in the secondary seeding, which would lead to the piling of more seeds at the end of the type hole and thereby greater seeding deviations.

Table 11 Test results of the effect of seeding plate speed on seeding performance

Rotation speed/r·min^{-1}	Pass rate/%	Missing rate/%	Repeating rate/%	Hole formation rate/%	Hole distance qualified rate/%
20	82.98	10.63	6.39	87.80	86.95
25	80.00	12.50	7.50	82.98	83.20
30	78.57	11.90	9.53	78.79	80.56

Table 12 Experiment results of different hole combinations

Various combinations	Average grain number per hole	Pass rate/%
Unilateral type hole	2.08	86.67
Unilateral type hole + unilateral suction hole	4.05	82.98
Unilateral type hole + bilateral suction hole	6.21	78.85
Bilateral type hole	4.97	78.57
Bilateral type hole + unilateral suction hole	6.43	73.91

2) Seeding performance of double-cavity combination

To test the performance of double-cavity synchronous seeding, bench tests were carried out on unilateral type hole and/or unilateral suction hole, unilateral type hole + bilateral suction hole, bilateral type hole + unilateral suction-hole, and bilateral type hole + bilateral suction hole, under the test conditions of 20 r/min seeding plate speed, negative pressure of air chamber –3600 Pa, 150 mm seed casting height, and 70 mm seed layer thickness. The test results are listed in Table 12.

The qualified rates of different combinations of type holes and suction holes were all higher than 70%, following the decreasing order of unilateral type hole, unilateral type hole + unilateral suction hole, unilateral type hole + bilateral suction hole, bilateral type hole, bilateral type hole + unilateral suction hole. With increasing number of type holes and suction holes in the combination, the average number of seeds per hole increases, indicating that this adjustable rice seed metering device can meet the sowing requirements of different rice varieties.

5.2 Field experiment

5.2.1 Evaluation index

According to the national standard NY/T 987-2006, field tests were carried out with the qualified rate, missing rate, and repeating rate as the test indices.

5.2.2 Test process

The rice-rape rotation field of Huazhong Agricultural University was used as the experimental field. After mechanical stubble treatment before the experiment, the average firmness of 20 cm deep soil was 6.93 kPa; the average moisture content of soil was 31.23%; and the experimental field area was 1.044 km^2.

The designed rice seed metering device was fixed on the seeding machine, and the traveling speed of the machine was 1.2 km/h. The field experiment is shown in Figure 21a. The negative pressure was provided by a fan, and the seeding shaft was powered by the ground wheel of the seeding machine. A total of

40 holes were continuously established, including five groups of tests. The seeding effect is shown in Figure 21b.

a. Field experiment

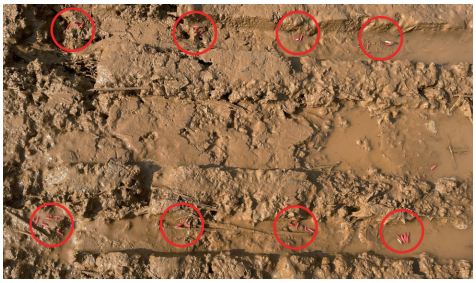

b. Seeding effect

Figure 21 Field experiment of rice seeding and effect

5.2.3 Test results of seeding amount regulation

The field test results of different combinations are shown in Table 13, in which A is for unilateral type hole, AB is for unilateral suction hole + unilateral type hole, and ABB is for unilateral suction hole + bilateral type.

Table 13 Seeding test data

Level	Test	Qualified rate/%	Missing rate/%	Repeating rate/%
1	A	70.0	12.5	17.5
2	A	67.5	12.5	20.0
3	AB	72.5	17.5	10.0
4	AB	82.5	12.5	5.0
5	ABB	65.0	25.0	10.0
6	ABB	67.5	22.5	10.0
7	AA	70.0	17.5	12.5
8	AA	72.5	15.0	12.5
9	AAB	67.5	20.0	12.5
10	AAB	60.0	25.0	15.0

The results of the field test show that when seeding of 1-3 seeds/hole was taken as qualified, the average qualified rate of unilateral type hole was 68.75%, the average missing rate was 12.5%, and the average repeating rate was 18.75%. When seeding of 3-6 seeds/hole was taken as qualified, the average qualified rate of unilateral type hole + unilateral suction hole was 77.5%, the average missing rate was 15.0%, and the average reseeding rate was 7.5%; the average qualified rate of bilateral type hole was 71.25%, the average missing rate was 16.25%, and the average reseeding rate was 12.5%. When seeding of 5-8 seeds/hole was taken as qualified, the average qualified rates of bilateral suction hole + unilateral type hole and bilateral type hole + unilateral suction hole were 63.75% and 66.25%, the average missing rates were 22.50% and 23.75%, and the average repeating rates were 13.75% and 10.00%, respectively. These results demonstrate that the designed rice seed metering device can achieve adjustable rice seeding amount. The error between the field test and the bench test is mainly due to two reasons: 1) The ground was uneven during the field test, and the seeding machine continuously generated vibration, thus affecting the seeding performance. 2) The seeding device was installed at a certain height from the ground during the field test, which increased the seed throwing height and affected the hole formation rate, thereby influencing the seeding performance.

6 Conclusions

To address the issues of narrow seeding adjustment range and low accuracy of grain placement in existing rice seeders, a combination-adjustable precision hole-type seeder was designed. Theoretical analyses of the seed charging, seed protection, and seed release processes were performed to determine the following parameters: seeding disk diameter of 192 mm, suction hole diameter of 1.48-1.52 mm, suction hole spacing of 3.04-9.41 mm, type hole distribution circle radius of about 62.1-77 mm, type hole diameter of 9 mm, stirrer plate length of 4.705-9.41 mm, and stirrer plate inclination angle of 0°-30°. This seeder allows for multi-level and multi-quantity adjustment of rice seeds by enabling the independent or simultaneous operation of mechanical and pneumatic seeding disks.

Using a coupled simulation method of EDEM-Fluent, the impact of type hole distribution, stirrer plate length, and inclination angle on seeding performance were analyzed. The results indicate that the primary and secondary factors affecting seed charging qualification rate are type hole diameter, stirrer plate inclination angle, and stirrer plate length. The optimal performance is achieved with a type hole diameter of 6 mm, stirrer plate length of 5 mm, and stirrer plate inclination angle of 10°, resulting in a seed charging qualification rate of 71.42%.

Furthermore, Fluent software was employed to analyze the influence of different suction hole spacings, diameters, and air chamber radii on seeding performance. The results show that a suction hole spacing of 6 mm, a suction hole diameter of 1.5 mm, an air chamber radius of 62 mm, and an average pressure of suction hole center of 2824.56 Pa could realize precise rice seed metering.

Bench tests and field tests for seeding quantity adjustment were conducted. The results show that for the single-chamber combination, the maximum seeding qualification rate is 82.5%, with a miss-seeding rate of 12.5% and a seedling formation rate of 71.79%. For the double-chamber combination, the maximum seeding qualification rate is 72.5%, with a miss-seeding rate of 15% and a seedling formation rate of 74.35%.

This combination-adjustable seeder offers a wide seeding adjustment range, high seeding precision, and superior seeding performance, effectively meeting the requirements for precision rice seeding of Huanghuazhan. In the future, combined with the physical characteristics of different varieties of rice, the sowing amount experiment of hybrid rice and conventional rice will be further optimized. These research findings can serve as a reference for the structural optimization of precision rice seeders.

Acknowledgements

This work was supported by the Outstanding Young and Middle-aged Science and Technology Innovation Team Program of Colleges and Universities of Hubei Province (Grant No. T201934), and the Development and Application of Rice and Camellia Fruit Mechanized Short Board Machine (Grant No. HBSNYT202208).

[References]

[1] Luo X W, Jiang E C, Wang Z M, Tang X R, Li J H, Chen W T. Precision rice hill-drop drilling machine. Transactions of the CSAE, 2008; 24(12):

52–56. (in Chinese)
[2] Liu W R, Zhang G Z, Zhou Y, Xu H M, Wu Q, Fu J W, et al. Application and development of intelligent technology in full mechanization of rice production. Journal of Huazhong Agricultural University, 2022; 41(1): 105–122. (in Chinese)
[3] Xing H, Wang Z M, Luo X W, He S Y, Zang Y. Mechanism modeling and experimental analysis of seed throwing with rice pneumatic seed metering device with adjustable seeding rate. Computers and Electronics in Agriculture, 2020; 178: 105697.
[4] Liu C B, Zang Y, Luo X W, Zeng S, Wang Z M, Yang W W, et al. Design and experiment of spiral grooved wheel for rice direct seeding machine. Journal of Shenyang Agricultural University, 2016; 47(6): 734739. (in Chinese)
[5] Li Z W, Shao Y J. Study and test of electromagnetic vibrating type rice seeder for hill seedling nursery box. Transactions of the CSAM, 2000; 31(5): 32–34. (in Chinese)
[6] Zhang M H, Luo X W, Wang Z M, Dai Y Z, Wang B L, Zheng L. Design and experiment of combined hole-type metering device of rice hill-drop drilling machine. Transactions of the CSAM, 2016; 47(9): 29–36. (in Chinese)
[7] Zhang G Z, Zhang S S, Yang W P, Lu K, Lei Z Q, Yang M. Design and experiment of double cavity side-filled precision hole seed metering device for rice. Transactions of the CSAE, 2016; 32(8): 9–17. (in Chinese)
[8] Xing H, Wang Z M, Luo X W, Zang Y, He S Y, Xu P, et al. Design and experimental analysis of rice pneumatic seeder with adjustable seeding rate. Int J Agric & Biol Eng, 2021; 14(4): 113–122.
[9] Zhang M H, Wang Z M, Luo X W, Jiang E C, Dai Y Z, Xing H, et al. Effect of double seed-filling chamber structure of combined type-hole metering device on filling properties. Transactions of the CSAE, 2018; 34(12): 8–15. (in Chinese)
[10] Ye Q. Design and experiment of a mechanical rice precision metering device with double cavity stirring hole. Master dissertation. Hubei: Huazhong Agricultural University, 2018. (in Chinese) doi: 10.7666/d.D01604001.
[11] Xu J, Sun S L, He Z K, Wang X M, Zeng Z H, Li J, et al. Design and optimisation of seed-metering plate of air-suction vegetable seed-metering device based on DEM-CFD. Biosystems Engineering, 2023; 230: 277–300.
[12] Zhao J L, Zhang C L, Wei Y P, Guo M Z, Chen C, Zhang C Q, et al. Design and testing of planting unit for rice dry-direct-seeding planter in cold region. Int J Agric & Biol Eng, 2023; 16(4): 76–84.
[13] Zhang G Z, Luo X W, Zang Y, Wang Z M, Zeng S, Zhou Z Y. Experiment of sucking precision of sucking plate with group holes on rice pneumatic metering device. Transactions of the CSAE, 2013; 29(6): 13–20. (in Chinese)
[14] Zhang M H, Xiao M, Ou Y L, Jiang E C, Qiao J, Wang Z M, et al. Optimization design and test of seed protecting structure of combined type-hole metering device. Journal of South China Agricultural University, 2021; 42(4): 99–105. (in Chinese)
[15] Tang H, Guan T Y, Xu F D, Xu C S, Wang J W. Test on adsorption posture and seeding performance of the high-speed precision dual-chamber maize metering device based on the seed characteristics. Computers and Electronics in Agriculture, 2024; 216: 108471.
[16] Du X, Liu C L. Design and testing of the filling-plate of inner-filling positive pressure high-speed seed-metering device for maize. Biosystems Engineering, 2023; 228: 1–17.
[17] Binelo M O, De Lima R F, Khatchatourian O A, Stránský J. Modelling of the drag force of agricultural seeds applied to the discrete element method. Biosystem Engineering, 2019; 178: 168–175.
[18] Tang H, Xu F D, Guan T Y, Xu C S, Wang J W. Design and test of a pneumatic type of high-speed maize precision seed metering device. Computers and Electronics in Agriculture, 2023; 211: 107997.
[19] Gao X J, Xie G F, Li J, Shi G S, Lai Q H, Huang Y X. Design and validation of a centrifugal variable-diameter pneumatic high-speed precision seed-metering device for maize. Biosystems Engineering, 2023; 227: 161–181.
[20] Zhang R F, Jiao W, Zhou J L, Qi B, Liu H, Xia Q Q. Parameter calibration and experiment of rice seeds discrete element model with different filling particle radius. Transactions of the CSAM, 2020; 51(S1): 227–235. (in Chinese)
[21] Shi S, Zhang D X, Yang L, Cui T, Li K H, Yin X W. Simulation and verification of seed-filling performance of pneumatic combined holes maize precision seed-metering device based on EDEM. Transactions of the CSAE, 2015; 31(3): 62–69. (in Chinese)
[22] Zhang G Z, Zang Y, Luo X W, Wang Z M, Li Z D. Line-churning tooth design and metering accuracy experiment of rice pneumatic precision hill-drop seed metering device on pregnant Japonica rice seed. Transactions of the CSAE, 2014; 30(17): 1–9. (in Chinese)
[23] Shen H, Zhang J J, Chen X H, Dong J X, Huang Y X, Shi J T. Development of a guiding-groove precision metering device for high-speed planting of soybean. Transactions of the ASABE, 2021; 64(3): 1113–1122.
[24] Li X L. Research on rice seed discharging device combined with spoon seed taking and piston hole insertion. Masterdissertation. Heilongjiang: Northeast Agricultural University, 2018. (in Chinese) doi: 10.7666/d.Y3430813.
[25] Zhai J B, Xia J F, Zhou Y. Design and experiment of pneumatic precision hill-drop drilling seed metering device for hybrid rice. Transactions of the CSAM, 2016; 47(1): 75–82. (in Chinese)
[26] Xue P, Xia X Y, Gao P Y, Ren D, Hao Y J, Hu B, et al. Double-setting seed-metering device for precision planting of soybean in high speed. Transactions of the ASABE, 2019; 62(1): 1–10.
[27] Yang W P. Research on the seed metering quality detection system of rice precision hole seeding metering device based on Labview. Master dissertation. Hubei: Huazhong Agricultural University, 2018. (in Chinese) doi: 10.7666/d.D01155272.
[28] Zhou Y, Hu M J, Xia J F, Zhang G Z, Xu Z Y, Feng C C, et al. Design and experiment of inside-filling adjustable precision seed-metering device with combined hole for cotton. Transactions of the CSAE, 2018; 34(18): 59–67. (in Chinese)